nature materials

REVIEW ARTICLE

PUBLISHED ONLINE: 22 APRIL 2014 | DOI: 10.1038/NMAT3921

Light management for photovoltaics using high-index nanostructures

Mark L. Brongersma[1]*, Yi Cui[1,2] and Shanhui Fan[3]

High-performance photovoltaic cells use semiconductors to convert sunlight into clean electrical power, and transparent dielectrics or conductive oxides as antireflection coatings. A common feature of these materials is their high refractive index. Whereas high-index materials in a planar form tend to produce a strong, undesired reflection of sunlight, high-index nanostructures afford new ways to manipulate light at a subwavelength scale. For example, nanoscale wires, particles and voids support strong optical resonances that can enhance and effectively control light absorption and scattering processes. As such, they provide ideal building blocks for novel, broadband antireflection coatings, light-trapping layers and super-absorbing films. This Review discusses some of the recent developments in the design and implementation of such photonic elements in thin-film photovoltaic cells.

Photovoltaic (PV) devices can effectively convert sunlight into clean electrical power and could provide a virtually unlimited amount of energy to our world. Crystalline Si (c-Si) solar cells[1] with thicknesses between 150–300 μm have dominated the market for decades and very high efficiency (~25% at one sun) cells of this material have been realized[2], and cells with efficiencies exceeding 22% are now sold commercially[3]. To expedite the large-scale implementation of PV technology, a tremendous amount of research has been devoted to reduce materials usage and the production cost of modules. Thin-film cells from a variety of semiconductor materials may provide a viable pathway towards this goal. Unfortunately, the energy-conversion efficiencies of such thin Si cells are at present substantially lower than their crystalline, wafer-based counterparts. This is a direct consequence of the large mismatch between the minority-carrier diffusion length and absorption depth in deposited thin-film materials, in particular near the bandgap. Effective photon management can address this issue and holds the promise of realizing ultrahigh-efficiency thin cells at low cost, the ultimate solution for the PV industry. Our continuously improving ability to absorb the same amount of sunlight in increasingly thin semiconductor layers directly leads to lower recombination currents, higher open circuit voltages and thus higher conversion efficiencies. Thin-film cells also alleviate the challenges associated with the scarcity of some solar-cell materials. Recently, major developments in high-efficiency III–V thin-film cells (a few 100 nm) and the potentially inexpensive production of ultrathin (5–20 μm) Si crystalline semiconductor wafers are also accelerating the development of thin cells. These include a variety of epitaxial lift-off processes and wafer-splicing techniques that employ etching, ion implantation and/or local stress generation techniques[4].

At present, it is not established which method of light trapping will be most successful for ultrathin cells and brute-force, full-field electromagnetic simulations are computationally too time intensive to identify the highest performance solutions in a vast design space. What has become clear is that the conventional macroscopic surface textures commonly applied on thick crystalline cells might not be suited for thin devices particularly when the cell thickness is comparable to or smaller than the macroscopic textures. Here, the implementation of nanostructured light-trapping layers is proving to be more effective[5]. The simplest light-trapping layers are realized by building solar cells on top of randomly textured substrates capable of redirecting incident sunlight into the plane of the semiconductor[6]. Such structures can now be synthesized by inexpensive, scalable deposition or etching techniques. To further improve our ability to trap light, it is important to understand which scattering nanostructures are optimal and how they are best arranged spatially on the cell surface. Based on their strong light concentration and scattering properties, light-trapping layers employing metallic (that is, 'plasmonic') nanostructures[7] have gained significant attention over the past decade although there are only a limited number of cases where the beneficial impact has been experimentally demonstrated on realistic cell designs[8,9]. In this Review, we focus our attention to high-refractive-index dielectric and semiconductor nanostructures. These structures feature a similar scattering albedo as metallic nanostructures without the parasitic optical losses.

This Review starts with a discussion on the basic science of light trapping in thin-film cells with the help of nanostructured light-trapping layers. It is argued that a 'wave optics' rather than a 'ray optics' perspective is required to analyse such cells and the limit to enhancing efficiency by light trapping is provided. This is followed by a discussion on how high-index nanostructures can be used to enhance absorption of sunlight by enabling the coupling to a variety of resonant modes of a solar cell. We then analyse the resonant modes of individual nanostructures and nanostructures placed into arrays to form novel types of antireflection coating (ARCs), light-trapping layers and super-absorbing films. We complete with a discussion of current efforts aimed at implementing such structures in realistic cells and new scalable patterning techniques that can produce structures over large areas in cost-competitive ways.

Fundamental light-trapping theory

The elucidation of a light-trapping limit in conventional, thick solar cells[10] has had a great influence on both our fundamental understanding of the thermodynamics of solar cells and on the practical design of light-trapping layers[11]. From a statistical ray optics analysis it follows that the maximum achievable absorption enhancement for a solar cell with an isotropic emission pattern is the Yablonovitch limit of $4n^2$, where n is the refractive index of the

[1]Geballe Laboratory for Advanced Materials, Stanford University, Stanford, California 94305, USA, [2]Stanford Institute for Materials and Energy Sciences, SLAC National Accelerator Laboratory, 2575 Sand Hill Road, Menlo Park, California 94025, USA, [3]Department of Electrical Engineering, Stanford University, Stanford, California 94305, USA. *e-mail: brongersma@stanford.edu

© 2014 Macmillan Publishers Limited. All rights reserved

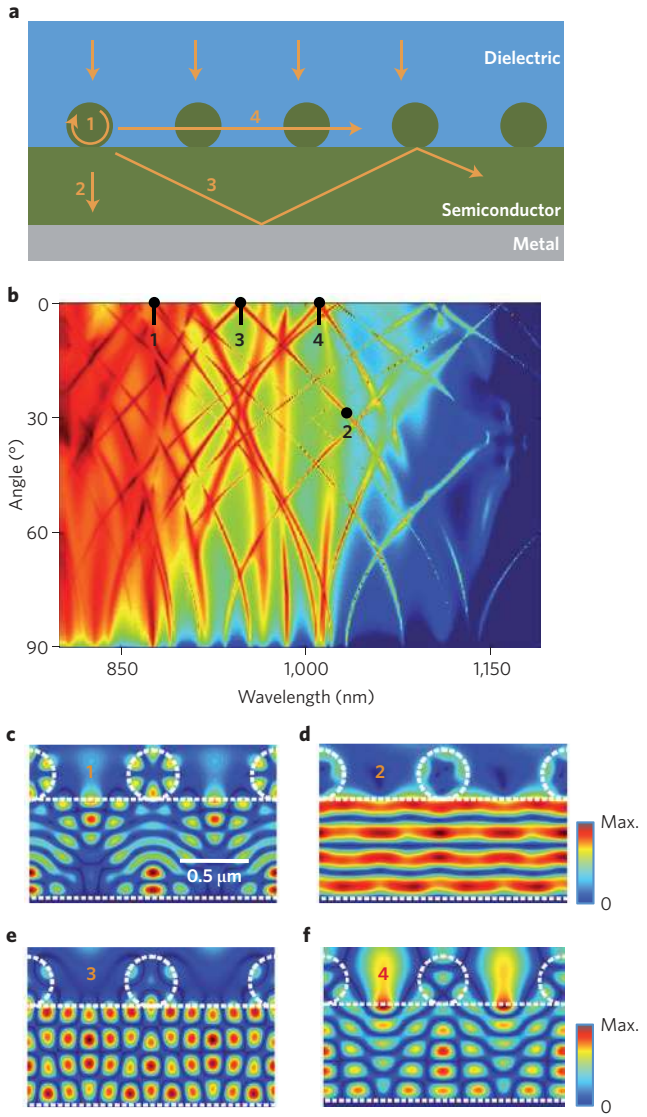

Figure 1 | Absorption enhancement caused by the excitation of optical resonances in a thin PV cell. a, Schematic showing how various optical resonances supported by a model cell structure can be excited to enhance light absorption in the active semiconductor material (green). The numbers 1–4 label four distinct coupling mechanisms. **b**, Simulated absorption as a function of the illumination wavelength and angle of incidence for a 1-μm-thick c-Si cell with a light-trapping layer consisting of a periodic array of c-Si nanowires. The numbers 1–4 label four specific illumination wavelength–angle pairs at which the coupling mechanisms illustrated in **a** are active. **c**–**f**, Electric-field-intensity distribution inside the cell for the four different illumination conditions (1–4) shown in **b**. The dashed white lines outline the c-Si structure. **c**, λ = 880 nm, normal incidence, showing the excitation of a mixture of a Mie resonance with a guided resonance. **d**, λ = 1,031 nm, 28° angle of incidence, showing the excitation of a Fabry–Perot resonance. **e**, λ = 946 nm, normal incidence, showing the excitation of a guided resonance in the Si layer. **f**, λ = 1,011 nm, normal incidence, showing a diffracted resonance by which a laterally propagating wave is excited in the light-trapping layer. Panels **b**–**f** courtesy of K. X. Wang.

absorbing semiconductor. When nanoscale photonic structures are used to manage solar photons in a thin cell, the conventional ray optics models break down and wave optics concepts are required to establish new performance limits. It is anticipated that a deep understanding of these limits and their origin can lead to the development of new, high-performance solar-cell designs.

In the wave-optics domain, one needs to start with an analysis of the electromagnetic modes of a solar cell[12–15]. A solar cell can support a great diversity of optical modes. Figure 1a illustrates this point with a schematic of a prototypical thin PV cell with a light-trapping layer consisting of high-index nanostructures. Specifically, it shows a 1-μm-thick c-Si film with a perfect back mirror and a light-trapping layer consisting of a periodic array of c-Si nanowires (NWs) on the top surface. Also shown are four of the most commonly occurring modes that can be excited to enhance light absorption in the spectral region where the cell is optically thin. The nature of these modes can be identified by plotting the light absorption in the semiconductor material as functions of the incident angle and illumination wavelength (Fig. 1b). The resulting two-dimensional absorption map shows a large number of features for which the absorption is strong. These features arise from the resonant coupling of sunlight to a multitude of distinct modes supported by the cell and are intuitively termed 'resonances'. Different types of resonance display different field distributions and exhibit different dependences of the resonance wavelength on angle (that is, different dispersive properties). These differences enable classification of the resonances. The labels 1–4 in Fig. 1b specify illumination conditions (angle and wavelength) with which the four resonances illustrated in Fig. 1a can be excited. The electric field distributions corresponding to these conditions are presented in Fig. 1c–f. Figure 1c clearly shows the excitation of an optical (Mie) resonance of hexapolar symmetry in the NWs. This resonance is hybridized with a guided resonance in the underlying Si layer. Figure 1d shows a low-quality-factor Fabry–Perot standing-wave resonance that results from the confinement of light between the reflecting top surface of the high-index Si film and the metallic back-reflector. Figure 1e shows a guided resonance of the Si layer[16]. It arises because the periodic NW-array can serve as a grating that ensures phase-matched coupling of a normally incident plane wave to a waveguided mode of the Si layer. The field distribution shows the periodic intensity variations in the plane of the semiconductor layer that are characteristic of guided resonances. Each guided resonance can uniquely be identified by overlaying the dispersion diagram of the various guided modes supported by the cell on top of the absorption map[17–19]. Another angle-dependent feature corresponds to the excitation of diffracted modes (Fig. 1f). Such modes can be excited when incident light is redirected into the plane of the light-trapping layer, where they concentrate most of the field[20]. These modes also extend into the underlying semiconductor layer where they can induce useful absorption. The ability to distinguish the different resonances together with knowledge on their origin enables a more thoughtful and effective optimization of the overall absorption of sunlight.

Each resonance features a characteristic linewidth that is governed by the time light spends/resonates in the cell. This time is limited by both the absorption in the semiconductor and radiation leakage back into the environment. From an examination of Fig. 1b, it is clear that all of the resonances have spectral linewidths that are much narrower than the solar spectrum. Therefore, to understand light trapping from a modal perspective, the aggregate contributions from each and every mode to the overall absorption enhancement needs to be assessed. The statistical temporal coupled-mode theory of Yu *et al.* provides a valuable formalism for this purpose[14]. The central idea is to calculate the total broadband absorption enhancement from all modes with the well-established temporal coupled-mode theory formalism.

The formulation of this type of light-trapping theory that is completely wave-optics-based yields important insights into the nature of the light-trapping process. In particular, the theory highlights the value of operating the different resonances in the strongly over-coupled regime that can be realized by enhancing the coupling in- and out of the absorber to the greatest extent possible.

© 2014 Macmillan Publishers Limited. All rights reserved

Although over-coupling leads to a reduced light absorption at the peak of a resonance, it enhances the broadband absorption by spectrally broadening the resonance. As such, it enables one to get the most out of each individual resonance and the optimal broadband absorption enhancement can be achieved by packing as many of such resonances per unit frequency. From a practical perspective, the statistical temporal coupled-mode theory can also be used to optimize the degree and type of disorder in light-trapping layers[21] as well as the angular emission/absorption properties[15,22,23] of cells. Experiments have proven the importance of optimizing these aspects of a solar cell[21,24–27].

The wave optics theory straightforwardly reproduces the classic $4n^2$ limit for a bulk cell. The theory also shows that a wavelength-scale thin film is subject to a limit that is very similar to the bulk limit[14], a fact that was noted earlier in ref. 13. Moreover, with the use of nanophotonic structures that enhance the density of optical modes over a broadband range of wavelengths, a light-trapping enhancement ratio significantly beyond the conventional limit can be achieved[14,28–31]. The theory can be generalized to situations where the material absorption is significant and again shows that the absorption enhancement beyond the conventional limit persists[32]. It is important to note that the wave optics theory presented here is consistent with the description of light trapping based on local density of optical states. Both theories account for the benefits of having a good mode overlap of the relevant modes with the absorbing medium[14,29].

Light trapping has conventionally been viewed as a way to enhance the short-circuit current of a solar cell by enhancing the photocarrier generation rate. As light-trapping strategies are becoming increasingly effective, ever thinner cells are considered where light management can also positively impact the open circuit voltage V_{oc}. In ultrathin absorber layers, the decreased bulk recombination can lead to a higher V_{oc} as this quantity increases with decreasing dark current I_{dark} as $V_{oc} = (kT/q)\ln(I_{photo}/I_{dark} + 1)$, where k is the Boltzman constant, T is the temperature of the cell, q is the absolute value of the electron charge and I_{photo} is the photocurrent. For cells with very low internal losses there are additional boosts possible in the V_{oc} (refs 33–35). This can be understood from an analysis of the work by Shockley and Queisser who explored all of the inevitable losses in a solar cell[36]. In this way, they were able to establish a limit to the efficiency for a single-junction cell. They demonstrated that very high efficiencies require a large product of electron–hole concentrations and effective fluorescent emission of photons from the cell. An explicit relationship between open circuit voltage and electroluminescence quantum efficiency was provided by Rau[37]. The latter requires extremely low internal losses as internally generated photons in a high-index semiconductor have a high probability to be trapped, re-absorbed and re-emitted. This process is termed 'photon recycling'. The observation of substantial external fluorescence is an indicator of low internal optical losses, which is a direct indication of the high-efficiency cell. To reach the Shockley and Queisser limit one needs to produce a cell with a 100% external fluorescence yield when the cell operates at the open-circuit voltage condition. It is thus clear that light-trapping strategies can be used to control both the current and the voltage of a solar cell[38], leading to new avenues for the enhancement of solar-cell performance.

High-refractive-index nanostructures

Insulating and semiconducting nanostructures provide a myriad of opportunities to manipulate light at the nanoscale. The higher their dielectric constant, the more strongly they tend to interact with incident sunlight. When properly sized and shaped, they can also exhibit very strong optical resonances that can further boost light–matter interaction compared with bulk materials. It is important to

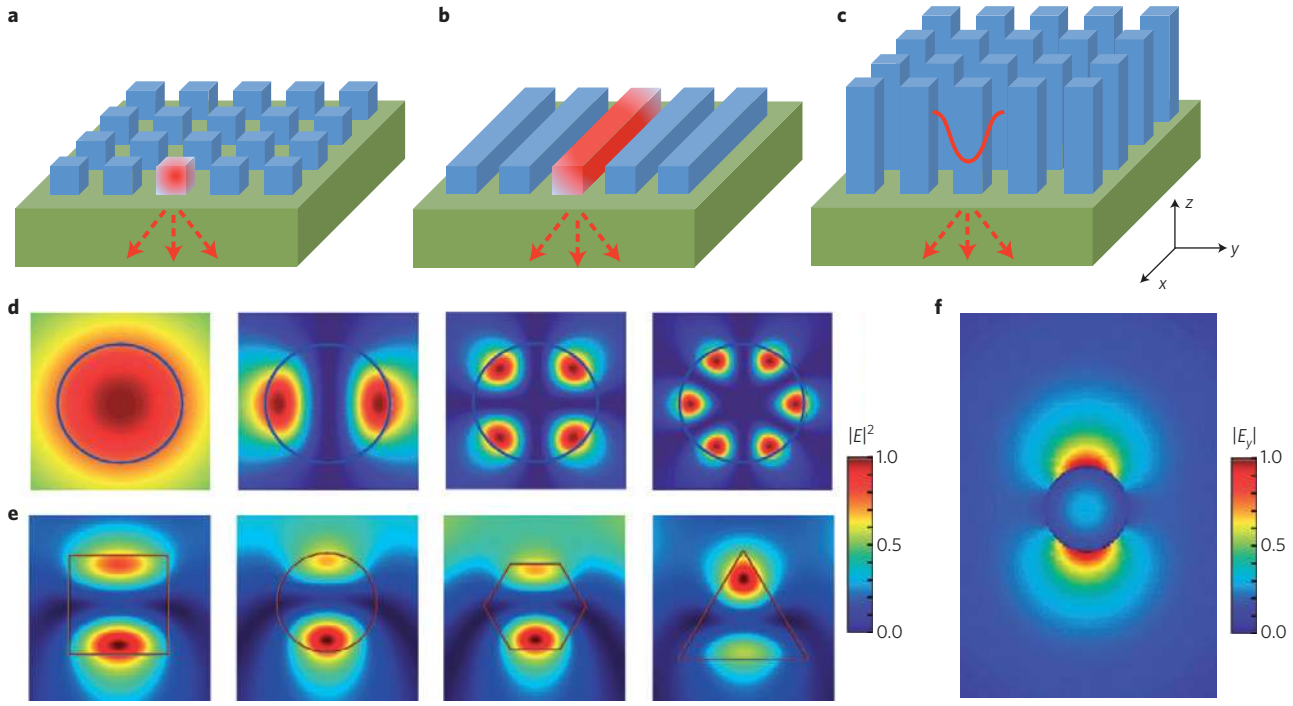

Figure 2 | Field distributions of the leaky optical modes supported by high-refractive-index nanostructures. a–c, Arrays of zero-dimensional nanoparticles (**a**), and one-dimensional nanowires oriented in a horizontal (**b**) or vertical (**c**) orientation (blue) placed on top of a solar cell (green). The red arrows depict the light scattering by the high-index nanostructures into the solar cell. **d**, Lowest-order transverse magnetic optical modes (m = 0, 1, 2, 3, shown from left to right) supported by subwavelength high-refractive-index nanocylinders. **e**, Electric field distributions inside subwavelength nanobeams of different cross-section shape for transverse magnetic illumination from above. The excitation wavelength was chosen to drive an m = 1 resonance. **f**, Major transverse electric field $|E_y|$ distribution of a fundamental HE_{11} mode of a 45-nm-radius silicon nanowire at a free-space wavelength of 547 nm. Figures reproduced with permission from: **d**, ref. 40, 2009 NPG; **e**, ref. 44, © 2010 ACS; **f**, ref. 46, © 2011 ACS.

© 2014 Macmillan Publishers Limited. All rights reserved

note that the strength of these resonances is similar to those found in metallic nanostructures[39]. They can also occur in deep-subwavelength structures (~10 nm) and have already enabled performance improvements of nanoscale optoelectronic devices that can densely be integrated with similar-sized semiconductor electronic components[40]. More recently, the PV community has started engineering these resonances with the aim to improve solar-cell performance. Excitation of these resonances in semiconductor nanostructures can directly increase the useful absorption if they are an integral part of the active solar cell material or indirectly by enabling excitation of guided and diffracted resonances. The way in which light is absorbed or scattered is determined by the nature of the localized optical resonances that can be excited in a nanostructure. To engineer the best possible ARCs and light-trapping layers, it is thus critical to classify the different types of localized resonance and to gain an intuitive understanding of their behaviour.

Figure 2a–c shows arrays composed of three of the most basic nanostructure types that can be employed to enhance light absorption in a solar cell. The arrays feature nanostructures that are zero-dimensional (that is, nanoparticles as shown in Fig. 2a) or one-dimensional (that is, NWs as shown in Fig. 2b,c). When illuminated from the top, localized optical resonances can be excited in the particles and horizontally oriented NWs that lie flat on a cell. These structures naturally confine the light in the propagation direction (z direction) and in at least one of the lateral directions (x and/or y directions). The vertically oriented wires can be extended many optical wavelengths and their properties can be most conveniently understood by first understanding their waveguiding properties.

The localized optical resonances supported by nanostructures that are small or comparable in size to the wavelength of light can be analysed following an approach originally taken by Gustav Mie[39]. Mie provided a solution to Maxwell's equations that describes the light scattering from a spherical particle. He decomposed the incident, scattered and internal electromagnetic fields into a basis set of vector spherical harmonics. The enforcement of boundary conditions on the particle surface then allowed for computation of the expansion coefficients of the scattered field. To describe the scattering from subwavelength particles of arbitrary shape, people have meritoriously performed a decomposition into a basis of multipolar functions. This is useful, because for such small particles the lowest-order multipoles (electric as well as magnetic dipoles and quadrupoles) will provide the dominant contributions to the scattered field. Many effective methods to calculate these contributions have been developed over the years[41,42]. Following this type of procedure, one can identify which resonant modes are excited in a structure. Each resonantly excited mode has a unique distribution of the electric and magnetic fields inside and around the particle and the extensive body of knowledge on these resonant modes can be leveraged in determining the best photon-management strategy.

To illustrate the nature of localized modes, we consider a simple example where one-dimensional scatterers (wires, beams and so on) are top-illuminated. In this case the resonances can be classified into purely transverse electric (electric field perpendicular to the length of the one-dimensional structure) or transverse magnetic (electric field parallel to the long axis)[43]. Furthermore, the modes can be indexed by an integer m that denotes the azimuthal phase dependence ($e^{im\varphi}$) of the fields. As an example, Fig. 2d shows the lowest-order transverse magnetic modes supported by high-refractive-index nanocylinders. In analysing the scattering properties of such NWs, it is helpful to view them as miniaturized versions of the well-established microcylinder resonators that can trap light in circulating orbits by multiple total internal reflections from the periphery. These are termed whispering gallery modes. Based on this viewpoint, it can be understood that resonances occur whenever an integer number m of wavelengths fits around the circumference of the wire.

The observation of multipolar antenna resonances is not limited to perfect cylindrical or spherical geometries and they are a general feature of high-index nanostructures. To illustrate this point, Fig. 2e shows the field distributions that result from the excitation of a low-order (m = 1) resonance in high-index beams of different cross-sectional shape. Such resonances can be excited in any semiconductor (Si, GaAs, CdTe, CIGS, organic)[44] and transparent oxides[20] with medium-to-high refractive indices. Even a nanoscale void in a high-index structure can support a resonance that can be exploited for light-trapping purposes[45]. The general occurrence of these resonances results in a tremendous flexibility in terms of the materials choice and methods of synthesis for patterned light-trapping layers. As such, high-index nanostructures serve as a valuable light-trapping platform.

For vertically oriented wires, light can couple into the supported waveguide modes from the top. For deep-subwavelength diameter wires, one only needs to consider the coupling to the allowed HE_{11} mode[46]. Figure 2f shows the field distribution in and around the wire when this mode is excited. A frequency-dependence in its excitation originates from a frequency-dependence of the guided mode diameter that governs the modal overlap with, and thus coupling to, an incident plane-wave. A frequency-dependent response for finite-sized wires can also originate from Fabry–Perot resonances along the length of the wire[47].

The effectiveness with which individual nanostructures absorb or scatter light can be quantified in terms of absorption and scattering cross-sections. The absorption cross-section is intuitively defined as: $\sigma_{abs} = W_{abs}/|S_{inc}|$, where W_{abs} is the power absorbed in the nanostructure and $|S_{inc}|$ is the power flow per unit area for an incident plane-wave. This quantity is given by $|S_{inc}| = ½c\varepsilon_0(\varepsilon_d)^{½}|E_0|^2$, where c is the speed of light, ε_d is the dielectric constant of the host medium, ε_0 is the vacuum permittivity and E_0 is the amplitude of the electric field of an incident light wave. The scattering cross-section is analogously defined as $\sigma_{sca} = W_{sca}/|S_{inc}|$, where W_{sca} is the scattered power. Energy conservation also allows one to define an extinction cross-section as the sum of the absorption and scattering cross-sections: $\sigma_{ext} = W_{ext}/|S_{inc}| = \sigma_{abs} + \sigma_{sca}$, where W_{ext} is the the total power removed from the incident light wave by both scattering and absorption. The extinction cross-section represents an effective area from which light is captured and subsequently absorbed or re-scattered. To assess the effectiveness of a structure to scatter or absorb light, these cross-sections are often normalized to its geometrical area σ_{geom}. The resulting dimensionless numbers are termed the absorption efficiency $Q_{abs} = \sigma_{abs}/\sigma_{geom}$ and scattering efficiency $Q_{sca} = \sigma_{sca}/\sigma_{geom}$. Efficiencies exceeding 1 indicate the presence of an 'antenna action' by which light is collected and concentrated from an area that is greater than its geometrical cross-section[48]. The application of light-scattering theory can set fundamental limits to the magnitude of the different cross-sections that ultimately constrain our ability to manage photons in different applications[49].

Figure 3 shows several experiments that illustrate and quantify the light scattering, guiding and absorption properties of individual high-index nanostructures. Figure 3a,b shows scanning electron microscopy images of two spherical Si nanostructures of different size (radii of 131 nm and 104 nm)[50]. The insets show dark-field light-scattering images of these nanoparticles and different colours (green and red) can clearly be observed. These images serve to visually demonstrate the pronounced scattering resonances that can be produced in subwavelength nanoparticles. In refs 44, 51 and 52 it is shown how the multiple peaks that can appear in light-scattering spectra can be uniquely attributed to excitation of the allowed electric and magnetic modes supported by these small particles. Figure 3c shows how these type of resonances can continuously be tuned across the entire visible spectrum[43]. Figure 3d,e shows that individual vertical silicon NWs can also feature tunable colours

© 2014 Macmillan Publishers Limited. All rights reserved

in bright-field optical imaging. These are related to the reduced reflection occurring over a narrow band of wavelengths where efficient coupling to optical waveguide modes is achieved[46]. Spectral reflection measurements on individual NWs show that the reflection dip redshifts with increasing NW diameter.

It is also possible to show how light absorption in an individual semiconductor nanostructure can be resonantly enhanced to increase the generation rate of photocarriers per unit volume. This was accomplished by electrically connecting individual Ge NWs to allow extraction of photocurrent[40,52]. The photocurrent generated by the wire is a direct measure of the light absorption in the semiconductor material. The photocurrent spectra taken from NWs with radii of 10 nm (black), 25 nm (blue) and 110 nm (red) are shown in Fig. 3f. Each spectrum shows a number of distinct peaks that are dependent on the NW size. These peaks do not appear in the spectral dependence of the intrinsic material absorption (inset to Fig. 3f) and result from optical resonances that can be tuned by the NW diameter, geometry and environment. These types of experiment showing the benefits of engineering optical resonances in semiconductor optoelectronic devices have opened up new pathways to substantially enhance the performance of solar cells with in-plane and vertically oriented NWs[44,53–56].

In the following sections it will be shown that the spacing and spatial arrangement of nanostructures is as critical as the optical properties of the nanostructures themselves. When the spacings are deep-subwavelength, effective media can be formed with an effective index between that of the high-index building blocks and their lower-index environment. For this reason, they can serve as effective ARCs. When the spacings are on the wavelength-scale, they enable effective grating-coupling to guided resonances and offer the possibility to realize photonic crystals.

Nanostructured antireflection coatings

When light passes the interface between two media with different, complex refractive indices n_1 and n_2, the reflected light intensity at normal incidence can be assessed from the reflectivity $R = [(n_1 - n_2)/(n_1 + n_2)]^2$. This equation predicts that a strong reflection occurs when light from the Sun tries to enter semiconductor materials that typically feature both a high real and imaginary part of the refractive index. For example, a polished Si wafer will reflect in excess of 30% of the incident photons across the visible and near-infrared range where the Sun emits most of its power. A common method for reducing the reflection is to add a quarter-wavelength-thick ARC with a real index equal to the geometric mean of the substrate and air indices[57]. For conventional c-Si cells, popular ARCs are thin transparent films of silicon dioxide ($n = 1.5$) or silicon nitride ($n = 2$)[58]. These simple ARCs only work well for a limited range of wavelengths and angles of incidence for which the backreflected wave is minimized due to destructive interference. A more broadband and angularly-independent reduction in the light reflection can be achieved by depositing a multilayer with a graded-index, but their processing can become complex and expensive[59].

A dense array of semiconductor nanostructures provides an alternative strategy to the realization of ARCs that can be both thin and highly effective across a broad wavelength and angular range. One important early discovery that stimulated research on this class of ARCs is the work by Bernhard in the late 1960s who discovered that the corneas of moth eyes have a structured surface that dramatically suppresses the reflection of light[60]. This led to a demonstration in the 1970s that reactively sputter-etched semiconductor surfaces can have textures that render the surface completely black[61]. Stevens and Cody developed a theory to explain this observation and showed that dense arrays of deep-subwavelength nanostructures on a surface can serve as effective media whose optical properties can gradually be varied to minimize reflection[62]. Rigorous coupled-wave analysis techniques were shown to effectively model the angular

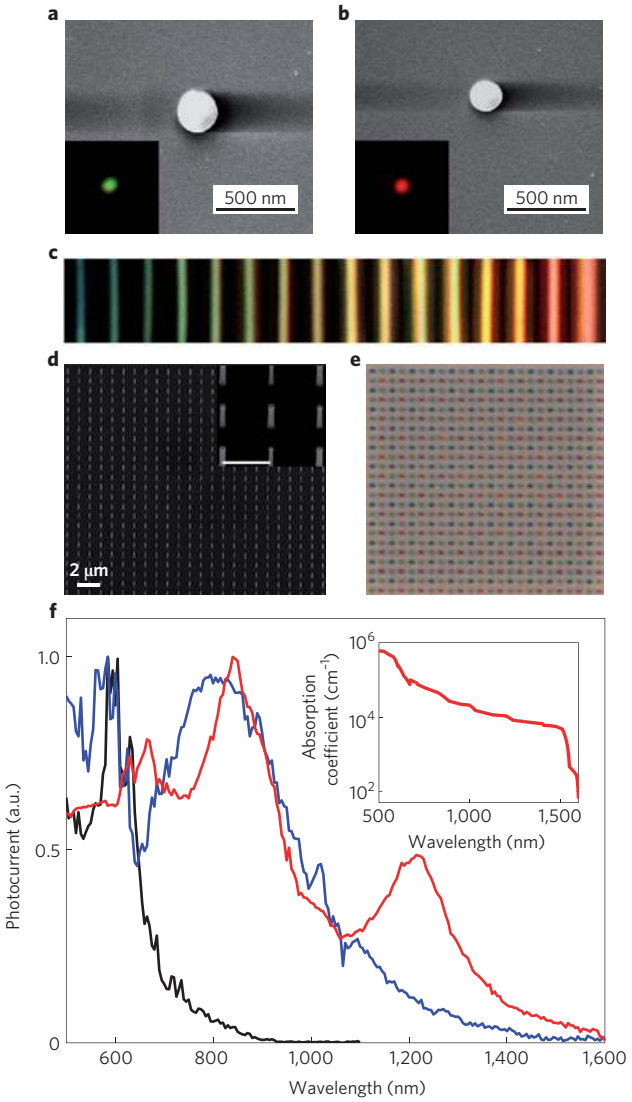

Figure 3 | Light scattering, guiding and absorption resonances of high-index nanostructures. a,**b**, Scanning electron microscope (SEM) images of spherical Si nanoparticles on a glass substrate with radii of $r \approx 131$ nm (**a**) and $r \approx 104$ nm (**b**). Insets show the corresponding dark-field light-scattering images of the particles. **c**, Dark-field light-scattering images of Si nanowires in the size range from 30 nm (blue) to 180 nm (red) under white light illumination. **d**, Tilted SEM image and magnified SEM image (inset, scale bar, 1 μm) of an array of Si nanowires with radii of 45, 50 and 65 nm. **e**, Bright-field optical microscope image showing the red, blue and green appearance of the differently sized wires shown in **d**. **f**, Measured photocurrent spectra taken from individual Ge nanowire photodetecors with radii of 10 nm (black), 25 nm (blue) and 110 nm (red). The spectra are normalized to the maximum value of the photocurrent. The inset shows the spectral dependence of the absorption coefficient of Ge. Figures reproduced with permission from: **a**,**b**, ref. 50, © 2012 ACS; **c**, ref. 43, © 2010 ACS; **d**,**e**, ref. 46, © 2011 ACS; **f**, ref. 40, 2009 NPG.

reflection properties of such materials[63]. Highly ordered arrays of subwavelength semiconductor nanostructures were first developed to suppress light reflection in the 1990s[63,64]. They could conveniently be generated over larger areas (~1 cm^2) by photolithographic means via plane-wave interference.

With the advances in nanofabrication techniques over the past decade, new procedures capable of generating graded or adiabatic refractive index changes over larger areas (~1 m^2) are now being developed at a rapid pace. Their implementation in thin solar

© 2014 Macmillan Publishers Limited. All rights reserved

cells is also becoming increasingly successful. Newly available nanostructuring techniques compatible with solar-cell fabrication include procedures for producing random textures via wet-chemical etching[65] as well as the synthesis of ordered-arrays of biomimetic Si nanotips[66], nanocones and domes[67,68], nanowires[69] and dual-diameter nanopillars[70]. Using amorphous Si (a-Si) as an example, Fig. 4a shows an array of nanocones patterned into a planar a-Si film by nanosphere lithography. The surface texture is capable of dramatically reducing the ~40% reflection from planar a-Si surface[67]. They were found to outperform nanopillar-arrays that reflect ~15% of the light by providing a more adiabatic index change from the air to the a-Si substrate index (Fig. 5b). The height, base diameter and aspect ratio of nanocones have been optimized to realize broadband, omnidirectional ARCs[68,71]. It was found that higher-aspect-ratio (>1) structures serve as the best ARCs and lower-aspect-ratio structures tend to scatter light more effectively and facilitate coupling to guided resonances of a solar cell. This and other types of light-trapping structure are discussed in more detail in the following sections. It is worth pointing out that cells with nanostructured surfaces are prone to performance degradation due to poor surface passivation. For this reason, it is interesting to note that thin dielectric overlayers on nanostructure arrays can further reduce reflection[72], hinting at the opportunity to realize dielectric passivation layers capable of also enhancing absorption[73]. Recent research is starting to show that very high power-conversion efficiencies can be obtained in cells with high-aspect-ratio nano- and microstructured semiconductor building blocks as long as the doping and surface passivation schemes are carefully designed to minimize the Auger and surface recombination[74,75].

Nanostructured light-trapping layers

One important direction of research and development in the PV community is the realization of ultrathin, low-cost solar cells that do not compromise on the high power-conversion efficiency of thick crystalline cells. This would be a great feat as optically thin cells typically only absorb a small fraction of the incident sunlight. The thinner the absorber layer, the more important it becomes to introduce an increasing number of coupling resonances capable of enhancing light absorption. This is particularly critical at long wavelengths as the absorption of light rapidly decreases with increasing wavelength towards the bandgap of a semiconductor. Adding nanostructures to a solar cell to strategically place such resonances across the solar spectrum constitutes the (art and) science of light trapping. If done well, there is an exciting opportunity to break the $4n^2$ limit[14,29]. Nanostructures can be positioned at the top and/or bottom surface of an absorber layer or the absorber layer itself can be nanostructured. The distinct benefits and challenges of these approaches are discussed below.

Nanostructures on the front surface of a cell. When structures are generated on the front surface, they can provide an effective pathway to couple light into a semiconductor layer and thereby reduce reflection. For example, the transparent conductive oxides used as electrical contacts in many solar cells can be roughened to attain some degree of light trapping[76]. Here, a careful engineering of the shape and size of such high-index nanostructures can enable coupling to localized Mie resonances capable of further enhancing the flow of light into the semiconductor. As the absorber layer typically has a higher index than the environment, the excitation of a Mie

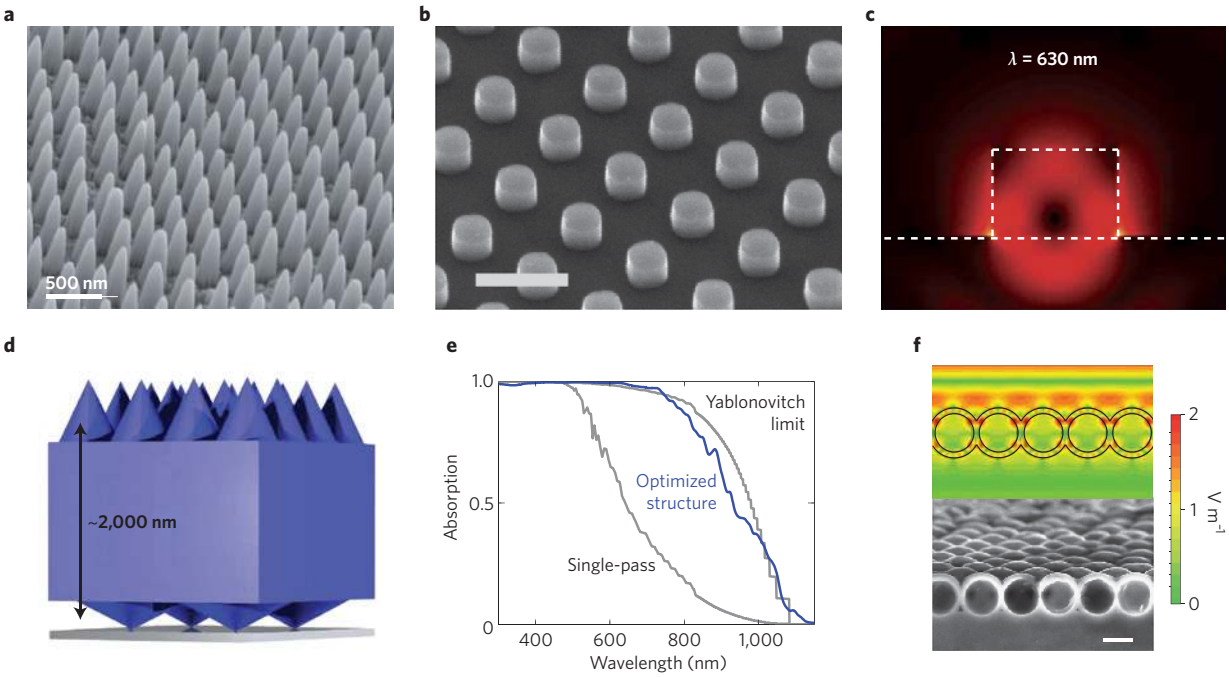

Figure 4 | Experimental realization of antireflection coatings with resonant, high-index nanostructures. a, SEM of an array of subwavelength nanocones on an a-Si solar cell. **b**, SEM image of 250-nm-diameter Si Mie scatterers on a Si substrate as generated by substrate-conformal imprint lithography. Scale bar, 500 nm. **c**, Full-field electromagnetic simulation of the electric-field-intensity distribution of a Mie resonance excited in a Si pillar like the ones shown in **b** with an in-plane diameter of 150 nm and height of 100 nm. The white dashed line shows the outline of the Si pillar and the substrate. **d**, Schematic of an ultrathin-film Si solar cell featuring a double-sided nanograting design, where the front and back surfaces of the cell were separately optimized for antireflection and light trapping, respectively. **e**, The spectral absorption of the optimized structure shown in **d**, where 1 corresponds to the case where all of the incident photons are absorbed. The optimized structure yields a photocurrent of 34.6 mA cm^{-2}, with an absorption enhancement close to the Yablonovitch limit. **f**, Bottom: SEM cross-sectional image of a monolayer of spherical Si nanoshells on a quartz substrate. Scale bar, 300 nm. Top: Full-field electromagnetic simulation of the electric-field distribution in the Si nanoshells shows the importance of the excitation of whispering gallery modes to enhance absorption of sunlight. Figures reproduced with permission from: **a**, ref. 67, © 2009 ACS; **b**,**c**, ref. 77, 2012 NPG; **d**,**e**, ref. 86, © 2012 ACS; **f**, ref. 94, 2012 NPG.

© 2014 Macmillan Publishers Limited. All rights reserved

resonance induces a preferential scattering into the absorber due to its higher mode density. Such a mechanism has been proposed to explain the effective trapping of light in a-Si cells with arrays of ZnO nanobeams[20] as well as the black appearance of single c-Si wafers patterned with arrays of nanoscale Si posts[77] (Fig. 4b). Optical simulations of these nanostructured surfaces clearly reveal the excitation of the Mie resonances, featuring a field distribution that extends into the higher-index absorber layer (Fig. 4c). This explains why the coupling to guided resonances of a solar cell can be very effective. It is also possible to realize light-trapping layers consisting of nanostructures supporting Mie resonances on top of already completely finished solar cells. For example, it has been demonstrated that placement of ordered arrays of dielectric spheres supporting Mie resonances could enhance the efficiency of a thin-film a-Si solar cell[78].

Nanostructuring at the back surface of a cell. Dielectric nanostructures at the back surface can be used as high-performance reflectors of light. For example, high-index dielectric nanoparticles of TiO_2 that make up white paint and sunscreen can form excellent, broadband backreflectors capable of redistributing light into guided resonances without the parasitic absorption of metallic backreflectors[79]. Such materials are low cost, earth abundant and environmentally friendly. More sophisticated, dielectric photonic crystals can also be made highly reflective across a targeted wavelength range[80–82]. When they are used as intermediate reflectors in serial-connected tandem cells, their spectral selectivity can be exploited to accurately balance currents from subcells[82,83].

Tuning of the exact shape and size of the nanostructures affords new levels of control over the angular and polarization distributions of the scattered light. A wide variety of dielectric nanostructure shapes, sizes and spacings have been explored to optimize light trapping and intuitive design rules are emerging[78,84,85]. Systematic nanophotonic simulations have been carried out to explore the possible benefits of nanostructuring both sides of an ultrathin c-Si solar cell as shown in Fig. 4d,e[86]. From this analysis, it was concluded that highly efficient light absorption can be obtained if high-aspect-ratio, dense (spacing ~500 nm) nanostructure-arrays are used in the front as an ARC and low-aspect-ratio lower-density nanostructure-arrays are used in the back to enable coupling to guided resonances. Here, the optimum structure spacing was found to be close to the target light-trapping wavelength: for a thin Si cell, the optimum periodicity of the nanocones was found to be 1,000 nm because light trapping is critical for the wavelength range from 800 to 1,100 nm, near the bandgap of Si.

Nanostructuring the absorber layer. Both the electronic and optical properties of a cell can benefit if the absorber layer is nanostructured. PV cells consisting of arrays of semiconductor nanowires with radial p–n junctions provide an excellent example of this point. The wire geometry offers effective radial charge extraction and excellent light absorption along the length of the wire[87–90]. This orthogonalization of carrier and photon transport enables lower-quality materials to be used with shorter minority-carrier diffusion lengths[91]. To achieve optimum performance requires a detailed joint optimization of the optical and electronic properties as both are strongly dependent on the geometry and size of the wire. The coupling of electronic and optical properties in nanostructured photonic devices is quite common and requires more complex opto-electronic simulation strategies[92].

Nano- and microstructured semiconductor layers can be turned into super-absorbing solar films by engineering the excitation of their local and guided resonances (Fig. 1). For example, instead of using nanocones as an ARC, one can create a nanostructured a-Si solar cell by depositing the active semiconductor material on top of a substrate patterned with nanocones[93]. The conformal deposition of ~300-nm-thick a-Si:H on top of the nanocones results in an active absorber layer with nanodomes. In this design, the nanodome shape not only provides gradual refractive index matching for antireflection but also couples the light into horizontally confined guided modes of the cell. Most of the light with wavelengths of 400 and 500 nm is absorbed in a single path through the a-Si:H layer and the antireflection effect is most important. The longer-wavelength photons (600 and 700 nm) are not absorbed in a single path and for those wavelengths the coupling to planar guided modes was maximized through an optimization of the dome spacing. The effective coupling leads to a weak reflection at these wavelengths.

It has been suggested that a solar-cell absorber layer can be built out of Mie resonators[44] and this was experimentally accomplished in an elegant way by Yao and colleagues[94]. They showed that nanocrystalline Si shells can be assembled into a solar cell that provides a 20-fold enhancement in the light absorption over a planar reference (Fig. 4f). It was shown that the coupling of light to the Mie modes of the shells produced a beneficial recirculation of the light waves in the absorber material. A key parameter in the optimization of this type of cell was a tuning of the optical quality factor of the resonators that governs the photon storage time. It was found that a relatively low-Q value of the Si nanoshell resonances not only allows efficient coupling between the incident light and resonant modes, but also spectrally broadens the resonant absorption enhancement region.

When the spacing of the nanostructures is on the wavelength scale, photonic-crystal effects can come into play as well. Studies aimed at optimizing the overall solar absorption have demonstrated the importance of a joint optimization of the nanostructure size, shape and filling ratio. One such study by Garnett *et al.* showed that an optimized cell with 5-μm-long Si nanowire arrays supported on an 8-μm-thick Si membrane could substantially increase the effective optical path length[95]. Photonic-crystal effects have systematically been studied in solar cells with the aim of increasing and spectrally tuning the local density of optical states within the absorber layer[29]. This brings the potential of exceeding the conventional ray optics light-trapping limit. Photonic-crystal solar cells have been realized by periodically arranging domes[93], holes[96,97] or wells[98] in thin-film cells. Other opportunities to enhance the local density of optical states can come about by exploiting localized or guided optical resonances in the nanostructures themselves[40,46,53,54,99].

Scalable fabrication over a large area

In order for high-index nanostructures to be applied in commercial PV technologies, their synthesis should be low-cost, high-yield and scalable. A common method for nanopatterning in industry is photolithography. This is a well-developed, widely used technique in the chip industry, but its use for low-cost manufacturing of solar cells remains to be developed. Below, several high-potential emerging nanopatterning techniques are presented.

Colloidal lithography uses two-dimensional arrays of colloidal nanospheres as a mask for further pattern transfer. In the past, silica and polymer nanospheres have been used to form monolayers through the Langmuir–Blodgett, spin-coating and dip-coating methods[100–102]. Although the throughput of these original methods is not high enough for solar-cell application, Jeong *et al.* developed a simple and scalable version[103]. They applied a wire-wound rod-coating method that is widely used for roll-to-roll processing in industry to deposit close-packed monolayers or multilayers of SiO_2 nanoparticles on a variety of rigid and flexible substrates (Fig. 5a). Such patterns can subsequently be transferred into light-trapping or semiconductor layers to realize nanowires or graded-index structures (Fig. 5b).

Another avenue involves combining inexpensive thin-film deposition and chemical processing of nanostructures. For example, the formation of high-index tin oxide (SnO_x) nanocones on various substrates was recently demonstrated on inexpensive substrates,

© 2014 Macmillan Publishers Limited. All rights reserved

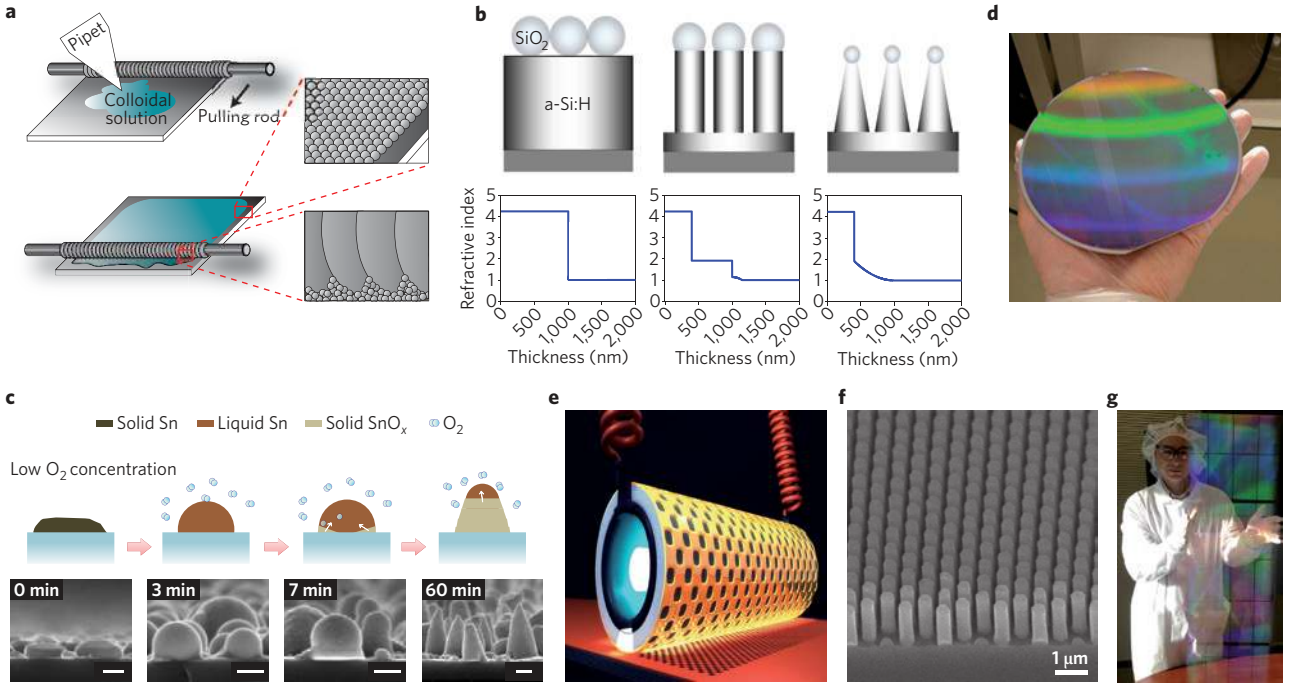

Figure 5 | Large-area nanopatterning techniques. a, Schematic explaining how a wire-wound rod-coating method can be applied to deposit close-packed monolayers or multilayers of SiO_2 nanoparticles on a variety of rigid and flexible substrates. The insets illustrate how the pulling rod evenly spreads the SiO_2 particles to form a close-packed layer on a surface. **b**, Illustration of how a SiO_2 nanoparticle array can be transferred into a Si substrate to form Si nanowires or cones with distinct refractive-index profiles. The bottom panels show the index profiles that can be achieved with the topologies shown in the top panels. **c**, Schematics and SEM images showing the formation of high-index tin oxide (SnO_x) nanocone arrays. All scale bars, 100 nm. **d**, Six-inch wafer with Si Mie scatterers made by substrate-conformal imprint lithography. **e**, Illustration of rolling-mask lithography, where a photoresist layer is illuminated with ultraviolet light through a rolling soft-mask wrapped around a quartz cylinder. **f**,**g**, SEM image of nanoscale pillars generated in silica glass by rolling-mask lithography (**f**), which can cover 1-metre-long glass panels (**g**). Figures reproduced with permission from: **a**, ref. 103, © 2010 ACS; **b**, ref. 67, © 2009 ACS; **c**, ref. 104, © 2011 ACS; **d**, ref. 106, courtesy of M. A. Verschuuren; **e**–**g**, ref. 107, courtesy of Rolith.

such as Si, aluminium foil, quartz and polyimide films, by a series of simple process steps: deposition and oxidation of a thin film of Sn in a low oxygen partial pressure (Fig. 5c)[104]. Annealing a thin film of Sn above its melting point (232 °C) in an inert gas environment with low oxygen concentration (less than 100 ppm) leads to the formation of liquid-phase Sn particles. When the Sn particles become supersaturated with dissolved oxygen, the solid SnO_x starts to nucleate at the interface between the liquid Sn and the solid substrate. The combined factors of high surface tension of the liquid-phase Sn and the consumption of Sn as SnO_x is formed results in the creation of tapered SnO_x nanocones. A variation of the processing parameters enables effective control over the SnO_x nanocone shape and thus allows tailored-made light-trapping coatings for different solar-cell designs.

Roll-to-roll nanoimprint lithography (NIL) offers another cost-effective nanopatterning technique[105]. It is based on mechanical deformation (thermal NIL) or curing (ultraviolet NIL) of resist materials. Although NIL enables generation of deep-subwavelength features, scaling of this technique to large areas remains a significant challenge. Substrate-conformal imprint lithography (SCIL) may facilitate scaling to larger areas in a cost-effective way[25,106]. This technique was used to generate the Mie scatterers shown in Fig. 4b and can already be applied to six-inch wafers (Fig. 5d). It has been used to realize nanostructures directly in SiO_2 and TiO_2 sol–gel layers or by pattern transfer in Si. A key step in this process is the creation of a polydimethylsiloxane rubber stamp that can be moulded from a Si master generated by electron-beam lithography. Recently, Rolith invented and developed another competing technology that enables the generation of nanoscale structures over large areas by optical lithography[107,108]. In the past, the use of phase-shift and near-field lithographic techniques over large areas was precluded due to the stringent requirements on air gaps between the photomask and a photoresist. Rolith circumvented these challenges by using a soft-mask wrapped around a quartz cylinder. A linear ultraviolet source placed within the cylinder illuminates the tie line between the cylinder and a substrate coated with photoresist (Fig. 5e). This facilitates exposure of the resist in a rolling fashion and enables patterning of subwavelength nanostructures (Fig. 5f) over metre-long panels (Fig. 5g). This process can effectively leverage the rapid developments in the fields of photolithography and nanophotonics to generate deep-subwavelength nanostructures and reduce cost. Both SCIL and the Rolith process benefit from the great aspects of soft lithography that enable patterning on non-planar substrates and afford substantial tolerance to particle contamination[109].

Outlook

This Review highlights the many approaches that can be taken in incorporating high-index nanostructures in solar cells. The ability of such structures to manipulate light at the subwavelength scale has sparked a wave of new research and development aimed at realizing the dream of ultrathin cells with efficiencies that can beat the traditional $4n^2$ limit. This wave encompasses new fundamental theory aimed at understanding the thermodynamics of thin cells. It involves development of new computational tools capable of operating in the wave optics domain, dealing with non-periodic structures, and performing joint electrical and optical optimization. It includes an elucidation of the light-absorption and scattering properties of subwavelength nanostructures in densely packed arrays placed on realistic solar cells and possibly with subwavelength spacings. Finally it tries to address the significant challenges in realizing such structures over large areas at low cost. The confluence of the dielectric nanophotonics, nanopatterning and solar fields may

© 2014 Macmillan Publishers Limited. All rights reserved

hold the key to realizing new, highly innovative solar cells that can provide high efficiency at extremely low cost.

Received 28 August 2013; accepted 20 February 2014; published online 22 April 2014

References

1. Green, M. A. The path to 25% silicon solar cell efficiency: history of silicon cell evolution. *Prog. Photovoltaics Res. Appl.* **17,** 183–189 (2009).
2. Green, M. A., Emery, K., Hishikawa, Y., Warta, W. & Dunlop, E. D. Solar cell efficiency tables (version 43). *Prog. Photovoltaics Res. Appl.* **22,** 1–9 (2014).
3. http://us.sunpowercorp.com/
4. Gordon, I. *et al.* Three novel ways of making thin-film crystalline-silicon layers on glass for solar cell applications. *Sol. Energy Mater. Sol. Cells* **95,** S2–S7 (2011).
5. Yu, Z., Raman, A. & Fan, S. Nanophotonic light-trapping theory for solar cells. *Appl. Phys. A* **105,** 329–339 (2011).
6. Krc, J., Smole, F. & Topic, M. Potential of light trapping in microcrystalline silicon solar cells with textured substrates. *Prog. Photovoltaics Res. Appl.* **11,** 429–436 (2003).
7. Atwater, H. A. & Polman, A. Plasmonics for improved photovoltaic devices. *Nature Mater.* **9,** 865–865 (2010).
8. Ferry, V. E. *et al.* Improved red-response in thin film a-Si:H solar cells with soft-imprinted plasmonic back reflectors. *Appl. Phys. Lett.* **95,** 183503 (2009).
9. Ding, I.-K. *et al.* Plasmonic dye-sensitized solar cells. *Adv. Energy Mater.* **1,** 52–57 (2011).
10. Yablonovitch, E. Statistical ray optics. *J. Opt. Soc. Am.* **72,** 899–907 (1982).
11. Campbell, P. & Green, M. A. Light trapping properties of pyramidally textured surfaces. *J. Appl. Phys.* **62,** 243–249 (1987).
12. Yablonovitch, E. & Cody, G. D. Intensity enhancement in textured optical sheets for solar cells. *IEEE Trans. Electron Dev.* **29,** 300–305 (1982).
13. Stuart, H. & Hall, D. Thermodynamic limit to light trapping in thin planar structures. *J. Opt. Soc. Am. A* **14,** 3001–3008 (1997).
14. Yu, Z., Raman, A. & Fan, S. Fundamental limit of nanophotonic light trapping in solar cells. *Proc. Natl Acad. Sci. USA* **107,** 17491–17496 (2010).
15. Yu, Z., Raman, A. & Fan, S. Fundamental limit of light trapping in grating structures. *Opt. Express* **401,** 397–401 (2010).
16. Fan, S. & Joannopoulos, J. Analysis of guided resonances in photonic crystal slabs. *Phys. Rev. B* **65,** 1–8 (2002).
17. Pala, R. A., White, J., Barnard, E., Liu, J. & Brongersma, M. L. Design of plasmonic thin-film solar cells with broadband absorption enhancements. *Adv. Mater.* **21,** 3504–3509 (2009).
18. Rockstuhl, C. & Lederer, F. Photon management by metallic nanodiscs in thin film solar cells. *Appl. Phys. Lett.* **94,** 213102 (2009).
19. Mokkapati, S., Beck, F. J., Polman, A. & Catchpole, K. R. Designing periodic arrays of metal nanoparticles for light-trapping applications in solar cells. *Appl. Phys. Lett.* **95,** 053115 (2009).
20. Vasudev, A., Schuller, J. & Brongersma, M. Nanophotonic light trapping with patterned transparent conductive oxides. *Opt. Express* **20,** 586–595 (2012).
21. Pala, R. A. *et al.* Optimization of non-periodic plasmonic light-trapping layers for thin-film solar cells. *Nature Commun.* **4,** 2095 (2013).
22. Campbell, P. & Green, M. A. The limiting efficiency of silicon solar cells under concentrated sunlight. *IEEE Trans. Electron Dev.* **33,** 234–239 (1986).
23. Yu, Z. & Fan, S. Angular constraint on light-trapping absorption enhancement in solar cells. *Appl. Phys. Lett.* **98,** 011106 (2011).
24. Rockstuhl, C., Lederer, F., Bittkau, K. & Carius, R. Light localization at randomly textured surfaces for solar-cell applications. *Appl. Phys. Lett.* **91,** 171104 (2007).
25. Ferry, V., Verschuuren, M. & Lare, M. Optimized spatial correlations for broadband light trapping nanopatterns in high efficiency ultrathin film a-Si: H solar cells. *Nano Lett.* **11,** 4239–4245 (2011).
26. Atwater, J. H. *et al.* Microphotonic parabolic light directors fabricated by two-photon lithography. *Appl. Phys. Lett.* **99,** 151113 (2011).
27. Martins, E. R., Li, J., Liu, Y., Zhou, J. & Krauss, T. F. Engineering gratings for light trapping in photovoltaics: The supercell concept. *Phys. Rev. B* **86,** 041404(R) (2012).
28. Green, M. A. Enhanced evanescent mode light trapping in organic solar cells and other low index optoelectronic devices. *Prog. Photovoltaics Res. Appl.* **19,** 473–477 (2011).
29. Callahan, D. M., Munday, J. N. & Atwater, H. A. Solar cell light trapping beyond the ray optic limit. *Nano Lett.* **12,** 214–218 (2012).
30. Munday, J. N., Callahan, D. M. & Atwater, H. A. Light trapping beyond the $4n^2$ limit in thin waveguides. *Appl. Phys. Lett.* **100,** 121121 (2012).
31. Schiff, E. A. Thermodynamic limit to photonic-plasmonic light-trapping in thin films on metals. *J. Appl. Phys.* **110,** 104501 (2011).
32. Yu, Z., Raman, A. & Fan, S. Thermodynamic upper bound on broadband light coupling with photonic structures. *Phys. Rev. Lett.* **109,** 173901 (2012).
33. Miller, O. D., Yablonovitch, E. & Kurtz, S. R. Strong internal and external luminescence as solar cells approach the Shockley–Queisser limit. *IEEE J. Photovoltaics* **2,** 303–311 (2012).
34. Niv, A., Gharghi, M., Gladden, C., Miller, O. D. & Zhang, X. Near-field electromagnetic theory for thin solar cells. *Phys. Rev. Lett.* **109,** 138701 (2012).
35. Polman, A. & Atwater, H. A. Photonic design principles for ultrahigh-efficiency photovoltaics. *Nature Mater.* **11,** 174–177 (2012).
36. Shockley, W. & Queisser, H. J. Detailed balance limit of efficiency of p-n junction solar cells. *J. Appl. Phys.* **32,** 510–519 (1961).
37. Rau, U. Reciprocity relation between photovoltaic quantum efficiency and electroluminescent emission of solar cells. *Phys. Rev. B* **76,** 085303 (2007).
38. Sandhu, S., Yu, Z. & Fan, S. Detailed balance analysis of nanophotonic solar cells. *Opt. Express* **21,** 1209–1217 (2013).
39. Bohren, F. & Huffman, D. *Absorption and Scattering of Light by Small Particles* (Wiley, 1983).
40. Cao, L. *et al.* Engineering light absorption in semiconductor nanowire devices. *Nature Mater.* **8,** 643–647 (2009).
41. Wriedt, T. *Generalized Multipole Techniques for Electromagnetic and Light Scattering* (Elsevier, 1999).
42. Evlyukhin, A. B., Reinhardt, C. & Chichkov, B. N. Multipole light scattering by nonspherical nanoparticles in the discrete dipole approximation. *Phys. Rev. B* **84,** 235429 (2011).
43. Cao, L., Fan, P., Barnard, E. S., Brown, A. M. & Brongersma, M. L. Tuning the color of silicon nanostructures. *Nano Lett.* **10,** 2649–2654 (2010).
44. Cao, L. *et al.* Semiconductor nanowire optical antenna solar absorbers. *Nano Lett.* **10,** 439–445 (2010).
45. Mann, S. A., Grote, R. R., Osgood, R. M. & Schuller, J. A. Dielectric particle and void resonators for thin film solar cell textures. *Opt. Express* **19,** 25729–25740 (2011).
46. Seo, K. *et al.* Multicolored vertical silicon nanowires. *Nano Lett.* **11,** 1851–1856 (2011).
47. Duan, X., Huang, Y., Agarwal, R. & Lieber, C. Single-nanowire electrically driven lasers. *Nature* **421,** 241–245 (2003).
48. Bohren, C. F. How can a particle absorb more than the light incident on it? *Am. J. Phys.* **51,** 323–327 (1983).
49. Schuller, J. A. & Brongersma, M. L. General properties of dielectric optical antennas. *Opt. Express* **17,** 24084–24095 (2009).
50. Evlyukhin, A. B. *et al.* Demonstration of magnetic dipole resonances of dielectric nanospheres in the visible region. *Nano Lett.* **12,** 3749–3755 (2012).
51. Kuznetsov, A. I., Miroshnichenko, A. E., Fu, Y. H., Zhang, J. & Luk'yanchuk, B. Magnetic light. *Sci. Rep.* **2,** 492 (2012).
52. Cao, L., Park, J.-S., Fan, P., Clemens, B. & Brongersma, M. L. Resonant germanium nanoantenna photodetectors. *Nano Lett.* **10,** 1229–1233 (2010).
53. Wallentin, J. *et al.* InP nanowire array solar cells achieving 13.8% efficiency by exceeding the ray optics limit. *Science* **339,** 1057–1060 (2013).
54. Krogstrup, P., Jørgensen, H. & Heiss, M. Single-nanowire solar cells beyond the Shockley–Queisser limit. *Nature Photon.* **7,** 306–310 (2013).
55. Kim, S.-K. *et al.* Tuning light absorption in core/shell silicon nanowire photovoltaic devices through morphological design. *Nano Lett.* **12,** 4971–4976 (2012).
56. Kempa, T. J. *et al.* Coaxial multishell nanowires with high-quality electronic interfaces and tunable optical cavities for ultrathin photovoltaics. *Proc. Natl Acad. Sci. USA* **109,** 1407–1412 (2012).
57. Zhao, J. & Green, M. A. Optimized antireflection coatings for high-efficiency silicon solar cells. *IEEE Trans. Electron Dev.* **38,** 1925–1934 (1991).
58. Zhao, J., Wang, A., Altermatt, P. & Green, M. A. Twenty-four percent efficient silicon solar cells with double layer antireflection coatings and reduced resistance loss. *Appl. Phys. Lett.* **66,** 3636–3638 (1995).
59. Xi, J.-Q. *et al.* Optical thin-film materials with low refractive index for broadband elimination of Fresnel reflection. *Nature Photon.* **1,** 176–179 (2007).
60. Berhard, C. G. Structural and functional adaption in a visual system. *Endeavor* **26,** 79–84 (1967).
61. Gittleman, J. I., Sichel, E. K., Lehmann, H. W. & Widmer, R. Textured silicon: A selective absorber for solar thermal conversion. *Appl. Phys. Lett.* **35,** 742–744 (1979).
62. Stephens, R. & Cody, G. Optical reflectance and transmission of a textured surface. *Thin Solid Films* **45,** 19–29 (1977).
63. Lalanne, P. & Morris, G. M. Antireflection behavior of silicon subwavelength periodic structures for visible light. *Nanotechnology* **8,** 53–56 (1997).
64. Wassermann, E. F. *et al.* Fabrication of large scale periodic magnetic nanostructures. *J. Appl. Phys.* **83,** 1753–1757 (1998).
65. Koynov, S., Brandt, M. S. & Stutzmann, M. Black nonreflecting silicon surfaces for solar cells. *Appl. Phys. Lett.* **88,** 203107 (2006).

© 2014 Macmillan Publishers Limited. All rights reserved

66. Huang, Y.-F. *et al.* Improved broadband and quasi-omnidirectional anti-reflection properties with biomimetic silicon nanostructures. *Nature Nanotech.* **2,** 770–774 (2007).
67. Zhu, J. *et al.* Optical absorption enhancement in amorphous silicon nanowire and nanocone arrays. *Nano Lett.* **9,** 279–282 (2009).
68. Jeong, S. *et al.* Hybrid silicon nanocone–polymer solar cells. *Nano Lett.* **12,** 2971–2976 (2012).
69. Tsakalakos, L. *et al.* Silicon nanowire solar cells. *Appl. Phys. Lett.* **91,** 233117 (2007).
70. Fan, Z. *et al.* Ordered arrays of dual-diameter nanopillars for maximized optical absorption. *Nano Lett.* **10,** 3823–3827 (2010).
71. Diedenhofen, S. L. *et al.* Broadband and omnidirectional anti-reflection layer for III/V multi-junction solar cells. *Sol. Energy Mater. Sol. Cells* **101,** 308–314 (2012).
72. Yu, Y., Ferry, V. E., Alivisatos, A. P. & Cao, L. Dielectric core-shell optical antennas for strong solar absorption enhancement. *Nano Lett.* **12,** 3674–3681 (2012).
73. Spinelli, P., Macco, B., Verschuuren, M. A., Kessels, W. M. M. & Polman, A. Al_2O_3/TiO_2 nano-pattern antireflection coating with ultralow surface recombination. *Appl. Phys. Lett.* **102,** 233902 (2013).
74. Oh, J., Yuan, H.-C. & Branz, H. M. An 18.2%-efficient black-silicon solar cell achieved through control of carrier recombination in nanostructures. *Nature Nanotech.* **7,** 743–748 (2012).
75. Kim, D. R., Lee, C. H., Rao, P. M., Cho, I. S. & Zheng, X. Hybrid Si microwire and planar solar cells: passivation and characterization. *Nano Lett.* **11,** 2704–2708 (2011).
76. Müller, J., Rech, B., Springer, J. & Vanecek, M. TCO and light trapping in silicon thin film solar cells. *Sol. Energy* **77,** 917–930 (2004).
77. Spinelli, P., Verschuuren, M. A. & Polman, A. Broadband omnidirectional antireflection coating based on subwavelength surface Mie resonators. *Nature Commun.* **3,** 692 (2012).
78. Grandidier, J., Callahan, D. M., Munday, J. N. & Atwater, H. A. Light absorption enhancement in thin-film solar cells using whispering gallery modes in dielectric nanospheres. *Adv. Mater.* **23,** 1272–1276 (2011).
79. Berger, O., Inns, D. & Aberle, A. G. Commercial white paint as back surface reflector for thin-film solar cells. *Sol. Energy Mater. Sol. Cells* **91,** 1215–1221 (2007).
80. Zeng, L. *et al.* Demonstration of enhanced absorption in thin film Si solar cells with textured photonic crystal back reflector. *Appl. Phys. Lett.* **93,** 221105 (2008).
81. Krc, J., Zeman, M., Luxembourg, S. L. & Topic, M. Modulated photonic-crystal structures as broadband back reflectors in thin-film solar cells. *Appl. Phys. Lett.* **94,** 153501 (2009).
82. Bielawny, A., Rockstuhl, C., Lederer, F. & Wehrspohn, R. B. Intermediate reflectors for enhanced top cell performance in photovoltaic thin-film tandem cells. *Opt. Express* **17,** 8439–8446 (2009).
83. Üpping, J. *et al.* in *Thin Film Solar Technology* (eds Delahoy, A. E. & Eldada, L. A.) *Proc. SPIE* Vol. 7409, 74090J (SPIE, 2009).
84. Mavrokefalos, A., Han, S. E., Yerci, S., Branham, M. S. & Chen, G. Efficient light trapping in inverted nanopyramid thin crystalline silicon membranes for solar cell applications. *Nano Lett.* **12,** 2792–2796 (2012).
85. Han, S. E. & Chen, G. Optical absorption enhancement in silicon nanohole arrays for solar photovoltaics. *Nano Lett.* **10,** 1012–1015 (2010).
86. Wang, K. X., Yu, Z., Liu, V., Cui, Y. & Fan, S. Absorption enhancement in ultrathin crystalline silicon solar cells with antireflection and light-trapping nanocone gratings. *Nano Lett.* **12,** 1616–1619 (2012).
87. Kayes, B. M., Atwater, H. A. & Lewis, N. S. Comparison of the device physics principles of planar and radial p-n junction nanorod solar cells. *J. Appl. Phys.* **97,** 114302 (2005).
88. Garnett, E. C. & Yang, P. Silicon nanowire radial p-n junction solar cells. *J. Am. Chem. Soc.* **130,** 9224–9225 (2008).
89. Kelzenberg, M. D. *et al.* Enhanced absorption and carrier collection in Si wire arrays for photovoltaic applications. *Nature Mater.* **9,** 239–244 (2010).
90. Garnett, E. C., Brongersma, M. L., Cui, Y. & McGehee, M. D. Nanowire solar cells. *Annu. Rev. Mater. Res.* **41,** 269–295 (2011).
91. Wangperawong, A. & Bent, S. F. Three-dimensional nanojunction device models for photovoltaics. *Appl. Phys. Lett.* **98,** 233106 (2011).
92. Deceglie, M. G., Ferry, V. E., Alivisatos, A. P. & Atwater, H. A. Design of nanostructured solar cells using coupled optical and electrical modeling. *Nano Lett.* **12,** 2894–2900 (2012).
93. Zhu, J., Hsu, C.-M., Yu, Z., Fan, S. & Cui, Y. Nanodome solar cells with efficient light management and self-cleaning. *Nano Lett.* **10,** 1979–1984 (2010).
94. Yao, Y. *et al.* Broadband light management using low-*Q* whispering gallery modes in spherical nanoshells. *Nature Commun.* **3,** 664 (2012).
95. Garnett, E. & Yang, P. Light trapping in silicon nanowire solar cells. *Nano Lett.* **10,** 1082–1087 (2010).
96. Park, Y., Drouard, E. & Daif, O. El. Absorption enhancement using photonic crystals for silicon thin film solar cells. *Opt. Express* **17,** 14312–14321 (2009).
97. Han, S. E. & Chen, G. Toward the Lambertian limit of light trapping in thin nanostructured silicon solar cells. *Nano Lett.* **10,** 4692–4696 (2010).
98. Leung, S.-F. *et al.* Efficient photon capturing with ordered three-dimensional nanowell arrays. *Nano Lett.* **12,** 3682–3689 (2012).
99. Fan, Z. *et al.* Three-dimensional nanopillar-array photovoltaics on low-cost and flexible substrates. *Nature Mater.* **8,** 648–653 (2009).
100. Jiang, P. & McFarland, M. J. Large-scale fabrication of wafer-size colloidal crystals, macroporous polymers and nanocomposites by spin-coating. *J. Am. Chem. Soc.* **126,** 13778–13786 (2004).
101. Huang, J., Kim, F., Tao, A. R., Connor, S. & Yang, P. Spontaneous formation of nanoparticle stripe patterns through dewetting. *Nature Mater.* **4,** 896–900 (2005).
102. Hsu, C.-M., Connor, S. T., Tang, M. X. & Cui, Y. Wafer-scale silicon nanopillars and nanocones by Langmuir–Blodgett assembly and etching. *Appl. Phys. Lett.* **93,** 133109 (2008).
103. Jeong, S. *et al.* Fast and scalable printing of large area monolayer nanoparticles for nanotexturing applications. *Nano Lett.* **10,** 2989–2994 (2010).
104. Jeong, S., McDowell, M. & Cui, Y. Low-temperature self-catalytic growth of tin oxide nanocones over large areas. *ACS Nano* **5,** 5800–5807 (2011).
105. Chou, S., Krauss, P. & Renstrom, P. Nanoimprint lithography. *J. Vac. Sci. Technol. B* **14,** 4129–4133 (1996).
106. Verschuuren, M. A. *Substrate Conformal Imprint Lithography for Nanophotonics* PhD thesis, Utrecht Univ. (2010).
107. http://www.rolith.com/
108. Kobrin, B., Barnard, E. S., Brongersma, M. L., Kwak, M. K. & Guo, L. J. in *Advanced Fabrication Technologies for Micro/Nano Optics and Photonics V* (eds Schoenfeld, W. V., Rumpf, R. C. & von Freymann, G.) *Proc. SPIE* Vol. 8249, 82490O (SPIE, 2012).
109. Xia, Y. & Whitesides, G. Soft lithography. *Annu. Rev. Mater. Sci.* **28,** 153–184 (1998).

Acknowledgements

The authors would like to acknowledge all of the students and postdocs in their groups who are actively involved with solar-energy research. We also greatly acknowledge support from the Center on Nanostructuring for Efficient Energy Conversion (CNEEC), an Energy Frontier Research Center funded by the US Department of Energy, Office of Science, Basic Energy Sciences under Award DE-SC0001060, DOE grant DE-FG02-07ER46426, and the Global Climate and Energy Project at Stanford University.

Additional information

Reprints and permissions information is available online at www.nature.com/reprints. Correspondence should be addressed to M.L.B.

Competing financial interests

M.L.B. is a co-founder of the company Rolith, which is one of the companies discussed in this Review that produces large-area nanostructured coatings.

© 2014 Macmillan Publishers Limited. All rights reserved